Validity of Small-Amplitude Oscillation Dynamic-Stability Measurement Technique

James C. Uselton* and B.L. Uselton†
ARO, Inc., Arnold Air Force Station, Tenn.

An investigation was conducted to evaluate the validity of the small-amplitude oscillation test technique for obtaining pitch-damping data. The effects of model oscillation frequency, oscillation amplitude, and sting length on pitch-damping characteristics were investigated for several configurations. Also, the pitch-damping data obtained by the small-amplitude forced-oscillation method were used in a six-degree -of-freedom computer program to predict decay motion from large amplitudes. These computed angular motions are compared with free decay motion measured on a free-oscillation gas bearing balance. The investigation was conducted at Mach number 3 and at a Reynolds number per ft of 4.73×10^6.

Nomenclature

A = reference area (based on reference length d), ft^2
C_m = pitching-moment coefficient, pitching moment $/q_\infty Ad$
C_{m_q} = $\partial C_m/\partial(qd/2V_\infty)$, damping-in-pitch derivative, 1/rad
$C_{m_{\dot\alpha}}$ = $\partial C_m/\partial(\dot\alpha d/2V_\infty)$, damping-in-pitch derivative, 1/rad
d = reference length: 1) maximum model diameter for cone models, 2) midbody cylinder diameter for cone-cylinder-flare model, ft
d_s = sting diameter, in. (at model base, 1.76 in.)
ℓ_s = effective sting length, in. (from model base to sting flare, see Fig. 2)
M_∞ = freestream Mach number
P_0 = tunnel stilling chamber pressure, psia
q = pitching velocity, rad/sec
q_∞ = freestream dynamic pressure, psia or psfa
R_b = model rounded base radius (see Fig. 1a), in.
Re/ft = freestream Reynolds number per ft
Re_d = freestream Reynolds number based on reference length d
r_b = model base radius, in.
T_0 = tunnel stilling chamber temperature, °R
V_∞ = freestream velocity, fps
α = angle of attack, deg
$\dot\alpha$ = time rate of change of angle of attack, rad/sec
θ = oscillation amplitude, deg
θ_{max} = maximum oscillation amplitude, deg
θ_c = model cone angle, deg
ω = oscillation frequency, rad/sec
$\omega d/2V_\infty$ = reduced frequency parameter, rad

Introduction

In recent years measurement of dynamic stability derivatives has become more refined and progressed to the state that small nonlinearities in damping trends with angle of attack can be measured. Personnel working with computer programs to predict vehicle trajectories and analyze their angular behavior have an increasing need for small-amplitude measurements because computer programs use instantaneous values. Therefore, in wind-tunnel testing the primary technique now being used to obtain basic pitch and yaw dynamic stability derivatives is the small-amplitude forced-oscillation technique. With the refinement of these measurements and more consistent use of the technique, questions now arise as to how well do these small-amplitude measurements apply to vehicles which have larger-amplitude excursions about their trim. Also, questions as to the importance and effect of oscillation frequency, oscillation amplitude, and sting effects have not been answered.

A research program was initiated in the von Karman Gas Dynamics Facility (VKF) at the Arnold Engineering Development Center (AEDC) to establish the validity of the small-amplitude dynamic stability test technique. Wind-tunnel tests were conducted in supersonic wind tunnel A of the VKF at Mach number 3 on a variety of model configurations.

Apparatus

Supersonic wind tunnel A in the VKF is a continuous-flow, closed-circuit, variable-density wind tunnel with an automatically driven, flexible-plate-type nozzle, and a 40x40-in. test section. The tunnel can be operated at Mach numbers from 1.5 to 6 at maximum stagnation pressures from 29 to 200 psia, respectively, and at stagnation temperatures up to 750°R.

Models

The stainless-steel models consisted of a 7-deg cone with and without a rounded base and a cone-cylinder flare with rounded base (CCFB) (Fig. 1). Bluntness ratios r_n/r_b of 0.0025 (sharp) and 0.15 were tested on the 8-in.-base-diameter conical model, and the rounded base radius R_b to model base radius r_b ratio was 0.5. The 7-deg model was fabricated so that ballast could be added to increase model inertia, and the combination of two model inertias and two cross-flexure balances gave four oscillation frequencies for the forced-oscillation tests. The maximum model inertia and minimum stiffness balance for the forced-oscillation tests were such that the wind on model frequency would be close to the frequency obtained when the model was tested on the gas bearing mechanism (free-oscillation tests).

The cone-cylinder-flare model had a midbody cylinder diameter of 5 in. and a rounded base radius to cylinder radius ratio of 1.42. Fabrication of this model was such that model

Presented as Paper 75-211 at the AIAA 13th Aerospace Sciences Meeting, Pasadena, Calif., January 20-22, 1975; submitted February 27, 1975; revision received November 10,1975. The research reported herein was conducted by the Arnold Engineering Development Center (AEDC), Air Force Systems Command. Research results were obtained by personnel of ARO, Inc., contract operator at AEDC. Further reproduction is authorized to satisfy needs of U.S. Government.

Index categories: LV/M Aerodynamics; LV/M System and Component Ground Testing.

*Section Supervisor, Aerodynamics Projects Branch, von Karman Gas Dynamics Facility. Associate Fellow AIAA.

†Project Engineer, Aerodynamics Projects Branch, von Karman Gas Dynamics Facility. Member AIAA.

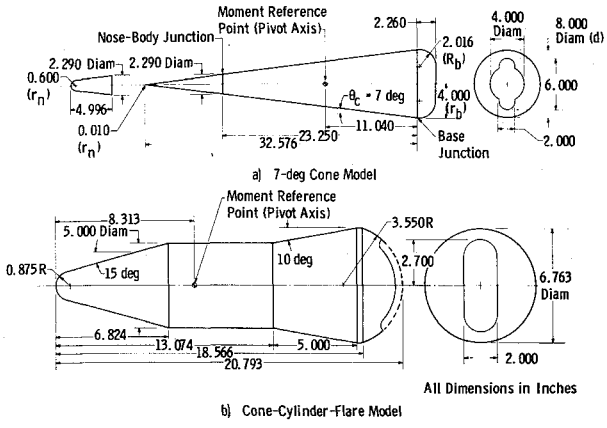

Fig. 1 Model details.

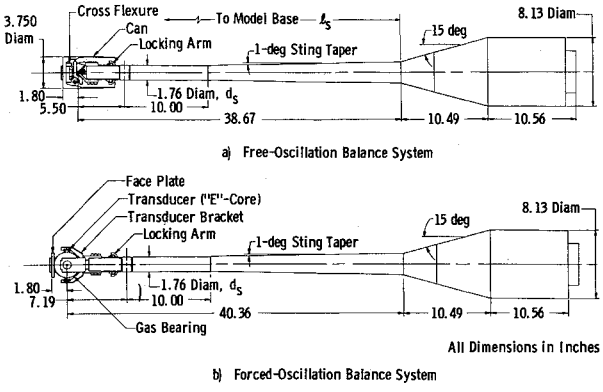

Fig. 2 Test mechanism details.

inertia could not be readily varied, and only two model frequencies were tested during the forced-oscillation tests. All models were balanced such that the model center of gravity was at the balance pivot axis. Geometric details are shown in Fig. 1.

Test Mechanisms

The test mechanisms (shown in Fig.2) utilized during the test program were a forced-oscillation balance and a free-oscillation balance. Information on these systems, their operation, and data reduction can be found in Refs. 1-3.

Both balances were supported by the same long, slender sting, which was designed and fabricated at VKF so that large effective sting lengths could be obtained which would eliminate or certainly minimize any sting interference effects. The effective sting length ℓ_s was approximately 3.5 cal for the flat base 7-deg model, and the sting diameter-to-model diameter ratio was 0.22. Figure 2 shows details of the two balances mounted to the sting. For the interference study, the effective sting length was shortened by positioning a flare at 1 and 1.5 cal to the rear of the model base (flat base). The flare was mounted to the motor housing so that it did not touch the sting forward of the motor housing. this eliminated the possibility of the flare changing the sting frequency characteristics or model tare damping.

Test Conditions

The test conditions were as follows: $M_\infty 3$, $p_0 = 31.84$ psia, $T_0 = 556°$R, $q_\infty = 5.416$ psia, $V_\infty = 2075$ fps, $Re/\text{ft} \times 10^{-1} = 4.73$.

Results and Discussion

Amplitude Effects

In the actual flight of most missiles,re-entry vehicles (R/V), and ballistic shells the vehicle will have only small-amplitude

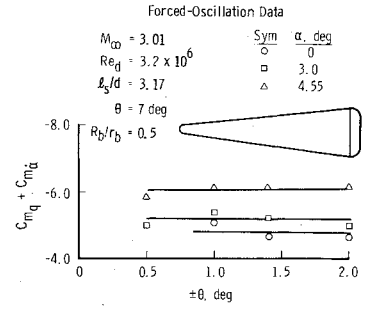

Fig.3 Effects of oscillation amplitude on pitch-damping coefficients.

excursions about some trim angle of attack. Typical flight trajectories have a maximum amplitude oscillation of approximately ±3.5 deg about the trim angle, and this only for very brief periods. Most of the time, the oscillation amplitudes of most vehicles are ±1 deg or less. Normally, in small amplitude testing, the model is oscillated approximately ±1 deg about different angles of attack. Therefore, in general, the small-amplitude test technique as used in this study would be directly applicable to the flight vehicle from a standpoint of oscillation amplitude.

Data were obtained on the 7-deg cone with the 0.15 nose bluntness and the rounded base for amplitudes ranging from 0.5 to 2.0 deg. These data (shown in Fig. 3) do not indicate any significant effect of amplitude. However, this is an area where more data are needed on more configurations before any general conclusions can be made. A simple analysis substantiates these findings, as it indicates at most a 5% change in angle for the time it takes the flow to pass over the body.

Effects of Oscillation Frequency

In conducting dynamic stability tests, the experimentalist normally attempts to match the flight frequency parameter $\omega d/2V_\infty$. However, many times because of certain mechanism restrictions, system natural frequencies, or because the flight range varies too much, the test program cannot be conveniently conducted at the desired frequency. When the test and flight frequency parameters are not matched, the question usually arises as to what effect does this have. Therefore, in this test program the models were tested at various frequencies.

The frequency investigation was conducted on the following 7-deg models: sharp nose with flat base, 0.15 nose bluntness with flat base, and the 0.15 nose bluntness with the rounded base. The data are presented in Figs. 4a-4c, respectively. The data for the cone-cylinder-flare model are presented in Fig. 4d. These results indicate no significant frequency effects for the cone configurations through the entire angle-of-attack range. The data for the cone-cylinder-flare model do indicate a measurable difference in the trends with angle of attack for the two different frequencies. It appears that the increased complexity of the flowfield of the cone-cylinder-flare body with its associated shocks, expansion waves, and possible separated region thus leads to frequency dependence. These data then indicate, although this study is not conclusive for all test conditions, that simple shapes such as sharp and blunt cones will not be frequency-dependent.

Sting Effects

The effect of the sting on dynamic stability test data has been of major concern in testing for many years. Many dynamic stability test mechanisms have a housing in the aft portion to enclose a motor or hydraulic system used to force the model (see Fig. 2). Thus, normally, the sting is straight coming out of the model and then at some point has a flare, which increases the diameter up to the housing. The flare can affect the wake closure of the model if it is sufficiently close to the model base. If this wake closure is affected, then the dynamic data can be influenced.

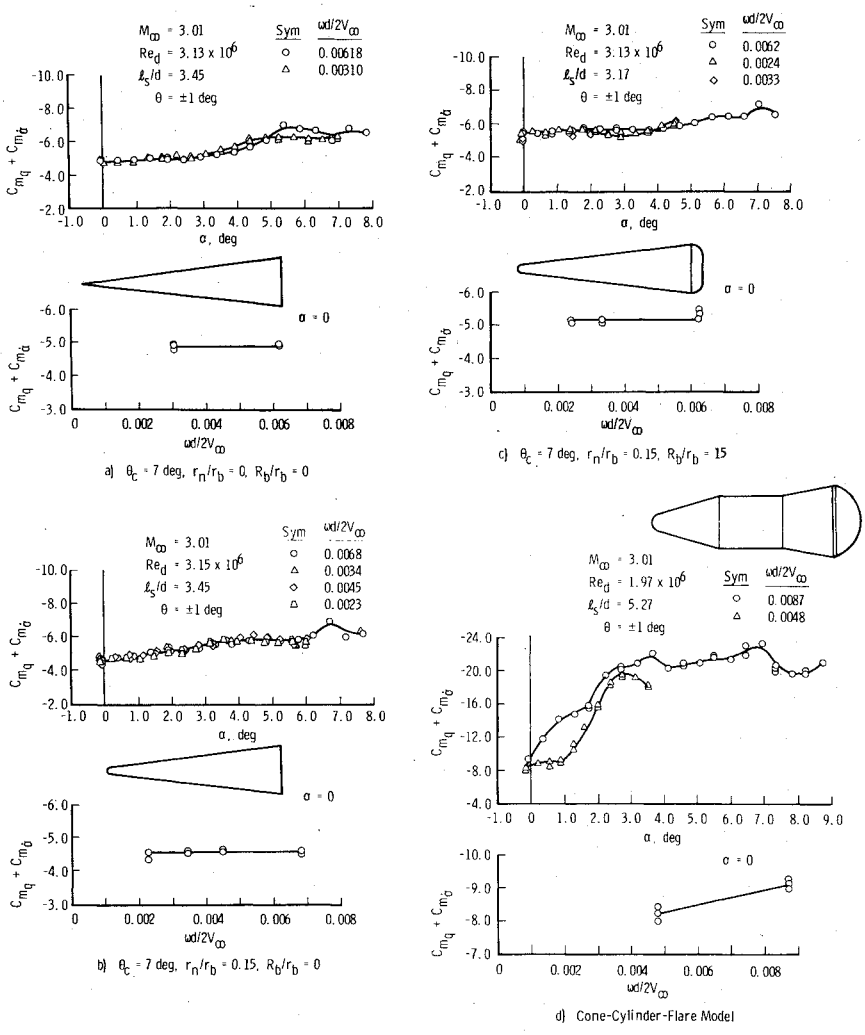

Fig. 4 Effects of oscillation frequency on pitch-damping coefficients.

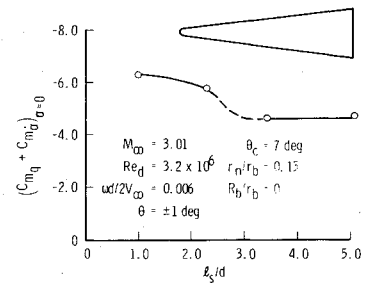

Fig. 5 Effect of sting length on pitch-damping coefficient.

The data shown in Fig. 5 illustrate the extent to which the sting length to the flare can influence the pitch damping on a sharp cone. These data show that when the sting length is decreased from 3.5 to 2.3 cal the damping increases. A sting length of 3.5 cal is evidently sufficient, as there is no change in the damping for an increase in sting length from 3.5 to 5.2 cal.

The sting interference effect is also shown in Figs. 6a-6c for $\omega d/2V_\infty$ equal to 0.0068, 0.0034, and 0.0023, respectively. These data indicate that the effect on pitch damping is most predominant at the lower angles of attack ($\alpha \leq 4$ deg). There tends to be little or no effect at the higher angles of attack. The static pitching-moment data C_m are shown to be independent of sting length (Figs. 6a-6c).

Also, these data indicate that the magnitude of the sting interference effect is dependent upon the frequency. This is best seen in Fig. 7, which shows the pitch-damping derivative versus $\omega d/2V_\infty$ for $\ell_s/d = 1.0$ and 3.5. As seen earlier, there is a considerable increase in damping caused by the sting flare at $\ell_s/d = 1$ at the higher frequencies. However, When the frequency is reduced so that $\omega d/2V_\infty = 0.0023$, there is little influence of sting length on damping at $\alpha = 0$. Therefore, experimentalists must be careful in conducting programs to ensure that damping trends with frequency are not really associated with sting interference. Sting bending can also influence the data and corrections must be applied.[3]

Computer Simulation Using Local Values

The objective of this portion of the study was to assess the validity of using small-amplitude measurements to predict angular vehicle motion by: 1) Measuring the pitch damping of various configurations over an angle-of-attack range using the small-amplitude (±2deg) forced-oscillation technique. 2) Mounting the same model on a one-degree-of freedom gas bearing and measuring the angular motion of the model when it is released from some initial amplitude (±6 deg) and allowed to decay ($t \lesssim 10$ sec). 3) Computing the angular motion of the models using the measured small-amplitude local-effective values from 1) together with the initial values of 2) in a standard six-degree-of-freedom computer program.

By then comparing the measured angular motion and the predicted angular motion, the applicability of using the small-amplitude damping values to predict actual vehicle angular motion can be evaluated. Various models were selected to obtain pitch-damping data that were constant, linear, and nonlinear with angle of attack. Limitations on available test time restricted this investigation to Mach number 3.

The experimental pitch-damping data are shown as a function of angle of attack in Figs. 8a-8d, for the three cone configurations and for the cone-cylinder-flare model. Also shown

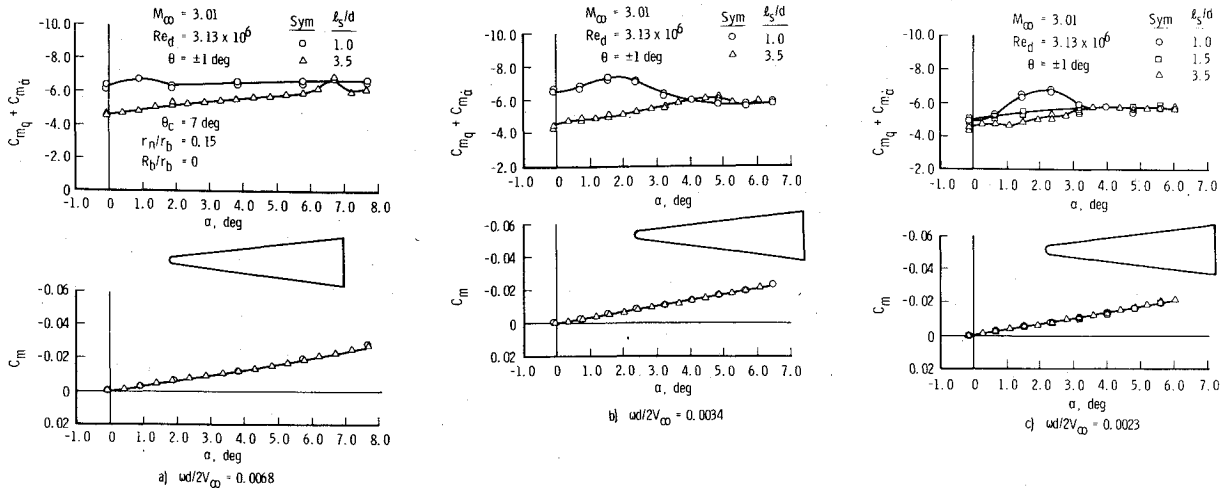

Fig. 6 Sting interference effects on pitch-damping and pitching-moment coefficients.

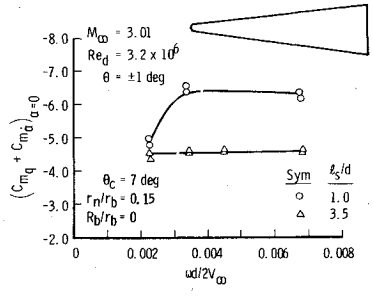

Fig. 7 Frequency effects on magnitude of sting interference.

are the faired curves of the local instantaneous values computed from the experimental local-effective values using the method of Ref. 4. The comparison of the experimental data and computed local values in Fig. 8 indicates that, generally the measured local-effective values compare closely with the instantaneous values and, therefore, the measured values could be used directly in the six-degree-of-freedom programs.

These local computed instantaneous damping values were then input into a six-degree-of-freedom computer program, along with the proper pitching-moment variation, initial amplitudes, ineritia, flow conditions, etc., and the motion was computed to compare with the motion measured by the one-degree-of-freedom-oscillation gas bearing test. The comparisons of the amplitude variation with time of the computer simulation using the small-amplitude data and of the acutal measured amplitude decay are shown in Fig. 9 for the different configurations. The comparison is seen to be excellent for the sharp cone, blunted cone, $r_n/r_b=0.15$, and blunted cone with the rounded base, $r_n/r_b=0.5$, and also for the cone-cylinder configuration. Thus, for a wide variety of configurations, the comparison indicates that the data obtained by the small-amplitude technique is certainly valid to use in trajectory analysis for studying vehicle motion.

Summary of Results

An investigation was conducted to evaluate the validity of the small-amplitude oscillation technique to measure vehicle pitch-damping characteristics. Tests were conducted at freestream Mach number equals 3.01 and freestream Reynolds number equals 3.13x10^6 and 1.97x10^6. A summary

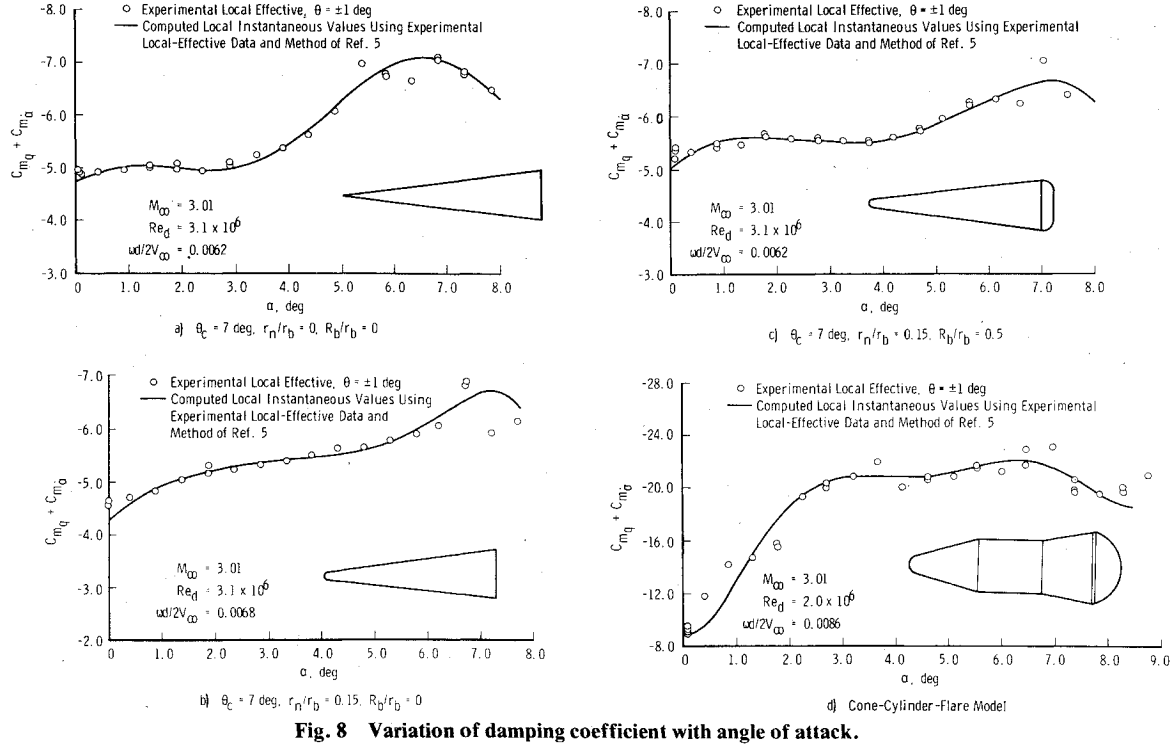

Fig. 8 Variation of damping coefficient with angle of attack.

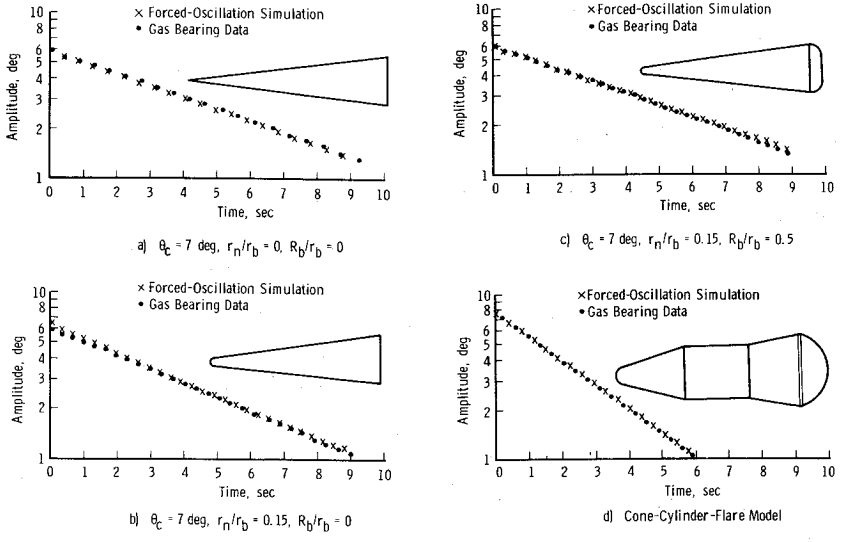

Fig. 9 Comparison of predicted amplitude decay using small-amplitude damping values to measured amplitude decay.

of the results of this investigation indicates the following: There was no evidence of amplitude (up to ±2 deg) effects on damping characteristics of the blunt cone with rounded base. On the cone configurations (sharp nose, blunt nose, and blunt nose with rounded base), there was no measurable effect of test frequency on damping characteristics. The damping characteristics of the cone-cylinder-flare model were frequency-dependent. The pitch damping on the blunt flat base cone increased when the effective sting length was decreased from 3.5 to 2.3 cal. The adverse effects of sting length on damping derivative were dependent on oscillation frequency.

The local-effective values measured by the small-amplitude forced-oscillation technique generally compare closely with instantaneous values calculated from the measured values. This indicated that the measured values may normally be substituted directly into six-degree-of-freedom computer programs to calculate vehicle motion.

For the three 7-deg cone configurations and the cone-cylinder-flare model, the amplitude decay predicted by the small-amplitude damping data matched the experimentally measured free-oscillation decay. Therefore, this result indicates that, for a wide variety of models, the small-amplitude data are valid for use in trajectory analysis of vehicle motion.

References

[1]Burt, G.E. "A Description of a Pitch/Yaw Dynamic Stability, Forced-Oscillation Test Mechanism for Testing Lifting configurations," Arnold Engineering Development Center, Arnold AFB, Tenn., AEDC-TR-73-60 (AD762286), June 1973.

[2]Schueler, C.J.,Ward, L.K., and Hodapp, A.E., Jr. "Techniques for Measurements of Dynamic Stability Derivatives in Ground Test Facilities."

[3]Burt, G.E. and Uselton, J.C. "Effect of Sting Oscillations on the Measurement of Dynamic Stability Derivatives in Pitch and Yaw," *Journal of Aircraft*, Vol. 13, March 1976, pp. 210-216.

[4]Billingsley, J.P. and Norman, W.S. "Relationship between Local and Effective Aerodynamic Pitch-Damping Derivatives as Measured by a Forced-Oscillation Balance for Preliminary Viking configurations," Arnold Engineering Development Center, Arnold AFB, Tenn. AEDC-TR-72-25 (AD741769), May 1972.